SUPPORTING DATA

G4LDB 2.2: a database for discovering and studying G-quadruplex and i-Motif ligands

Yu-huan Wang[1, †], Qian-Fan Yang[1, †], Xiao Lin[1], Die Chen[2], Zhi-yin Wang[1], Bing Chen[1], Hua-yi Han[2], Hao-Di Chen[1], Kai-Cong Cai[3], Qian Li[4], Shu Yang[2], *, Feng Li[1], *, Ya-Lin Tang[4], *

SUPPORTING DATA

Table S1 Representation of the active sites for docking models

Entry ID	Ligand site	Description	Grid box center (coordinate)	Grid ball radius (Å)	Site representation
1L1H	1	Crystal Structure of the Quadruplex DNA-Drug Complex	x: 17.276 y: 17.744 z: 7.802	15	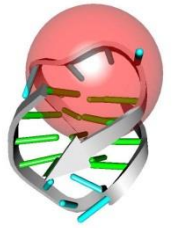
1O0K	1	Structure of the First Parallel DNA Quadruplex-drug Complex	x: 12.708 y: -5.04 z: 19.795	15	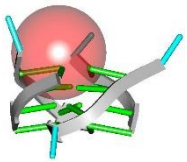
1O0K	2	Structure of the First Parallel DNA Quadruplex-drug Complex	x: 15.905 y: 6.504 z: 13.337	15	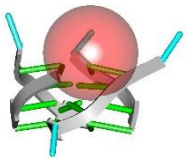

SUPPORTING DATA

1O0K	3	Structure of the First Parallel DNA Quadruplex-drug Complex	x: 19.292 y: -4.868 z: 7.144	15	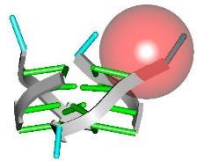
1NZM	1	NMR structure of the parallel-stranded DNA quadruplex d(TTAGGGT)4 complexed with the telomerase inhibitor RHPS4	x: 29.171 y: 35.136 z: 18.012	15	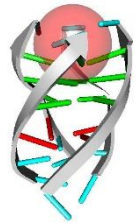
1NZM	2	NMR structure of the parallel-stranded DNA quadruplex d(TTAGGGT)4 complexed with the telomerase inhibitor RHPS4	x: 27.729 y: 29.372 z: 30.696	15	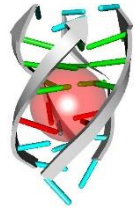
2A5R	1	Complex of tetra-(4-n-methylpyridyl) porphin with monomeric parallel-stranded DNA tetraplex, snap-back 3+1 3' G-tetrad, single-residue chain reversal loops, GAG triad in the context of GAAG diagonal loop, C-MYC promoter, NMR, 6 struct.	x: 2.689 y: 6.015 z: -5.483	15	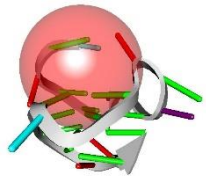

SUPPORTING DATA

2HRI	1	A parallel stranded human telomeric quadruplex in complex with the porphyrin TMPyP4	x: -18.602 y: -11.651 z: -15.251	15	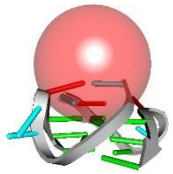
2HRI	2	A parallel stranded human telomeric quadruplex in complex with the porphyrin TMPyP4	x: -9.873 y: 0.156 z: -0.082	15	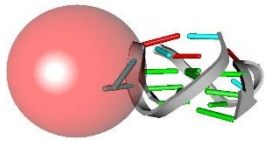
2JT7	1	NMR solution structure of the 4:1 distamycin A/[d(TGGGGT)]4 complex	x: 10.67 y: -0.132 z: 0.088	15	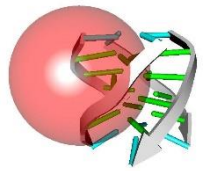
2JT7	2	NMR solution structure of the 4:1 distamycin A/[d(TGGGGT)]4 complex	x: 7.369 y: -2.298 z: 0.31	15	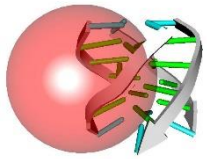

SUPPORTING DATA

2JWQ	1	G-quadruplex recognition by quinacridines: a SAR, NMR and Biological study	x: -5.532 y: -2.952 z: 21.319	15	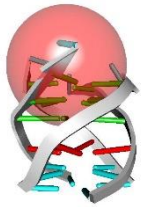
2JWQ	2	G-quadruplex recognition by quinacridines: a SAR, NMR and Biological study	x: -4.195 y: 1.861 z: 9.1	15	
2KVY	1	NMR solution structure of the 4:1 complex between an uncharged distamycin A analogue and [d(TGGGGT)]4	x: 33.63 y: 18.831 z: 36.73	15	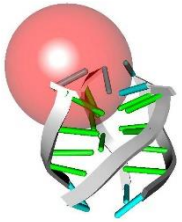
2KVY	2	NMR solution structure of the 4:1 complex between an uncharged distamycin A analogue and [d(TGGGGT)]4	x: 36.359 y: 22.394 z: 34.504	15	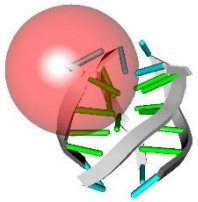

SUPPORTING DATA

2L7V	1	Quindoline/G-quadruplex complex	x: -1.351 y: -0.019 z: 2.804	15	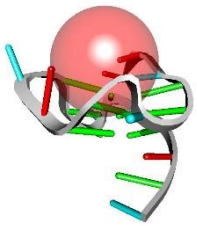
2L7V	2	Quindoline/G-quadruplex complex	x: -1.264 y: -5.934 z: -10.339	15	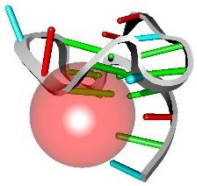
2MB3	1	Solution structure of an intramolecular (3+1) human telomeric G-quadruplex bound to a telomestatin derivative	x: 39.873 y: 30.281 z: 35.738	15	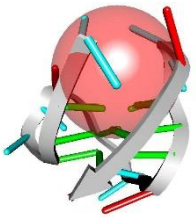
2MCC	1	Structural studies on dinuclear ruthenium(II) complexes that bind diastereoselectively to an anti-parallel folded human telomere sequence	x: -2.071 y: -6.804 z: -1.093	15	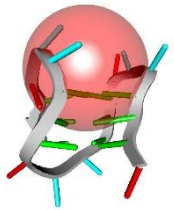

SUPPORTING DATA

2MCO	1	Structural studies on dinuclear ruthenium(II) complexes that bind diastereoselectively to an anti-parallel folded human telomere sequence	x: 38.3 y: 21.485 z: 29.993	15	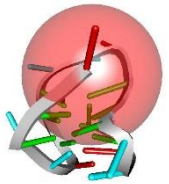
2MGN	1	Solution structure of a G-quadruplex bound to the bisquinolinium compound Phen-DC3	x: 36.402 y: 44.936 z: 35.387	15	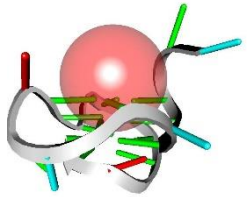
2MS6	1	Human Telomeric G-quadruplex DNA sequence (TTAGGGT)4 complexed with Flavonoid Quercetin	x: 10.69 y: 3.033 z: -1.282	15	
2MS6	2	Human Telomeric G-quadruplex DNA sequence (TTAGGGT)4 complexed with Flavonoid Quercetin	x: -9.953 y: -1.505 z: -2.866	15	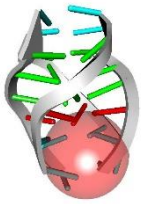

SUPPORTING DATA

2N6C	1	Solution structure for quercetin complexed with c-myc G-quadruplex DNA	x: 0.933 y: 0.356 z: 7.91	15	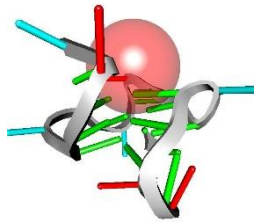
2N6C	2	Solution structure for quercetin complexed with c-myc G-quadruplex DNA	x: -2.63 y: 1.436 z: -6.926	15	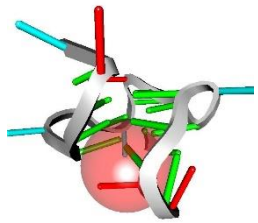
3CE5	1	A bimolecular parallel-stranded human telomeric quadruplex in complex with a 3,6,9-trisubstituted acridine molecule BRACO19	x: 17.985 y: 18.088 z: 9.447	15	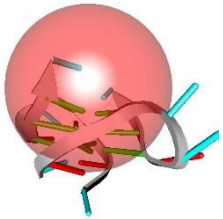
3CDM	1	Structural adaptation and conservation in quadruplex-drug recognition	x: 3.614 y: 12.255 z: -22.198	15	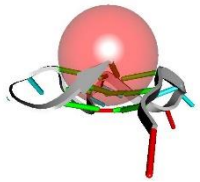

SUPPORTING DATA

3CDM	2	Structural adaptation and conservation in quadruplex-drug recognition	x: 2.63 y: 0.82 z: -14.778	15	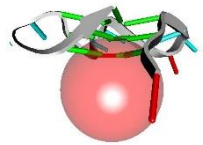
3EM2	1	A bimolecular anti-parallel-stranded Oxytricha nova telomeric quadruplex in complex with a 3,6-disubstituted acridine BSU-6038	x: 17.312 y: 17.848 z: 7.801	15	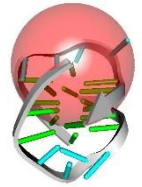
3EQW	1	A bimolecular anti-parallel-stranded Oxytricha nova telomeric quadruplex in complex with a 3,6-disubstituted acridine BSU-6042 in small unit cell	x: 10.296 y: -3.23 z: -8.135	15	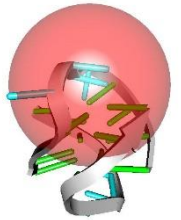
3ERU	1	A bimolecular anti-parallel-stranded Oxytricha nova telomeric quadruplex in complex with a 3,6-disubstituted acridine BSU-6045	x: 10.307 y: -3.362 z: -7.942	15	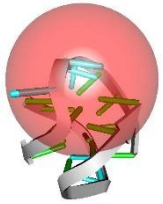

SUPPORTING DATA

3ES0	1	A bimolecular anti-parallel-stranded Oxytricha nova telomeric quadruplex in complex with a 3,6-disubstituted acridine BSU-6048	x: -10.137 y: 2.587 z: -7.78	15	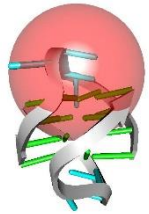
3ET8	1	A bimolecular anti-parallel-stranded Oxytricha nova telomeric quadruplex in complex with a 3,6-disubstituted acridine BSU-6054	x: 17.319 y: 18.167 z: 8.09	15	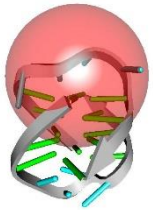
3EUI	1	A bimolecular anti-parallel-stranded Oxytricha nova telomeric quadruplex in complex with a 3,6-disubstituted acridine BSU-6042 in a large unit cell	x: -6.889 y: -3.18 z: 5.511	15	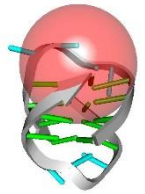
3EUM	1	A bimolecular anti-parallel-stranded Oxytricha nova telomeric quadruplex in complex with a 3,6-disubstituted acridine BSU-6066	x: 17.504 y: 18.115 z: 8.209	15	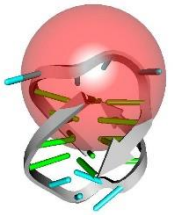

SUPPORTING DATA

3NYP	1	A bimolecular anti-parallel-stranded Oxytricha nova telomeric quadruplex in complex with a 3,6-disubstituted acridine ligand containing bis-3-fluoropyrrolidine end side chains	x: 18.164 y: 18.525 z: 8.135	15	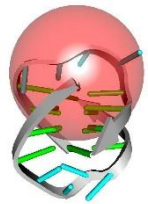
3NZ7	1	A bimolecular anti-parallel-stranded Oxytricha nova telomeric quadruplex in complex with a 3,6-disubstituted acridine ligand containing bis-3-fluoropyrrolidine end side chains	x: 17.427 y: 17.988 z: 7.86	15	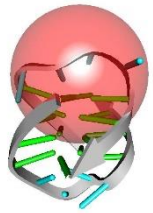
3R6R	1	Structure of the complex of an intramolecular human telomeric DNA with Berberine formed in K+ solution	x: 16.55 y: 27.836 z: 4.416	15	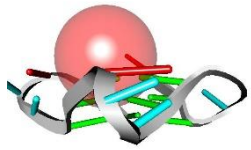
3R6R	2	Structure of the complex of an intramolecular human telomeric DNA with Berberine formed in K+ solution	x: 16.553 y: 28.01 z: -2.948	15	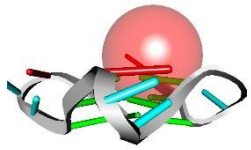

SUPPORTING DATA

3R6R	3	Structure of the complex of an intramolecular human telomeric DNA with Berberine formed in K+ solution	x: 4.526 y: 21.157 z: -1.52	15	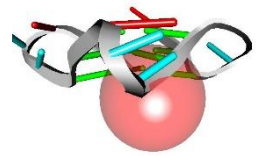
3R6R	4	Structure of the complex of an intramolecular human telomeric DNA with Berberine formed in K+ solution	x: 2.723 y: 26.184 z: 3.24	15	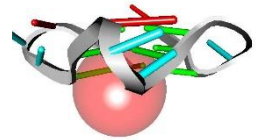
3SC8	1	Crystal structure of an intramolecular human telomeric DNA G-quadruplex bound by the naphthalene diimide BMSG-SH-3	x: -17.969 y: -13.586 z: 8.007	15	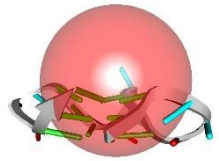
3T5E	1	Crystal structure of an intramolecular human telomeric DNA G-quadruplex bound by the naphthalene diimide BMSG-SH-4	x: -22.581 y: 6.872 z: -9.713	15	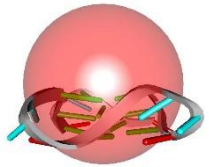

SUPPORTING DATA

3UYH	1	Crystal structure of an intramolecular human telomeric DNA G-quadruplex bound by the naphthalene diimide compound, MM41	x: -2.691 y: -22.446 z: -7.872	15	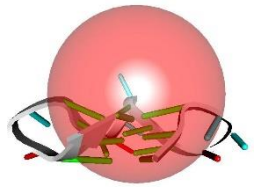
4DA3	1	Crystal structure of an intramolecular human telomeric DNA G-quadruplex 21-mer bound by the naphthalene diimide compound MM41	x: 18.114 y: -13.41 z: 0.52	15	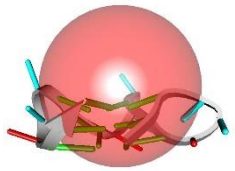
4DAQ	1	Crystal structure of an intramolecular human telomeric DNA G-quadruplex 21-mer bound by the naphthalene diimide compound BMSG-SH-3	x: 17.758 y: 13.207 z: 7.868	15	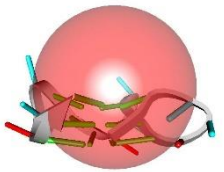
4FXM	1	Crystal structure of the complex of a human telomeric repeat G-quadruplex and N-methyl mesoporphyrin IX (P21212)	x: -5.373 y: 10.823 z: -1.049	15	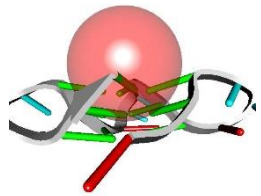

SUPPORTING DATA

4G0F	1	Crystal structure of the complex of a human telomeric repeat G-quadruplex and N-methyl mesoporphyrin IX (P6)	x: 8.42 y: 46.985 z: -1.579	15	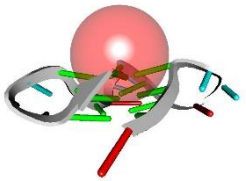
4P1D	1	Structure of the complex of a bimolecular human telomeric DNA with Coptisine	x: -1.644 y: -21.422 z: -11.925	15	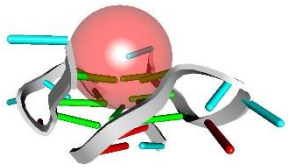
4TS0	1	Crystal structure of the Spinach RNA aptamer in complex with DFHBI, barium ions	x: 29.027 y: 24.936 z: 15.935	15	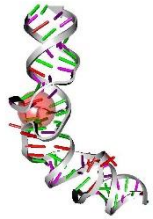
4TS2	1	Crystal structure of the Spinach RNA aptamer in complex with DFHBI, magnesium ions	x: -5.286 y: -2.085 z: -10.12	15	

SUPPORTING DATA

5BJO	1	Crystal structure of the Corn RNA aptamer in complex with DFHO, site-specific 5-iodo-U	x: 3.729 y: 9.948 z: -13.402	15	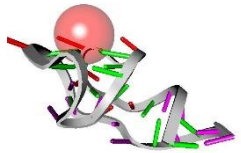
5BJP	1	Crystal structure of the Corn RNA aptamer in complex with DFHO, iridium hexammine soak	x: 3.953 y: -10.139 z: -85.407	15	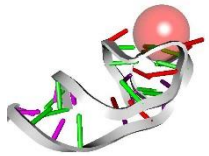
5CCW	1	Structure of the complex of a human telomeric DNA with Au(caffein-2-ylidene)2	x: -0.984 y: 12.947 z: -17.128	15	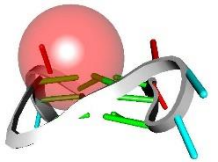
5CCW	2	Structure of the complex of a human telomeric DNA with Au(caffein-2-ylidene)2	x: -1.386 y: 12.968 z: -9	15	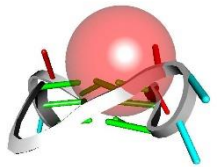

SUPPORTING DATA

5CCW	3	Structure of the complex of a human telomeric DNA with Au(caffein-2-ylidene)2	x: -3.5 y: 0.019 z: -14.685	15	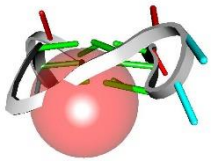
5CDB	1	Structure of the complex of a bimolecular human telomeric DNA with a 13-diphenylalkyl Berberine derivative	x: 0.266 y: -19.945 z: 5.942	15	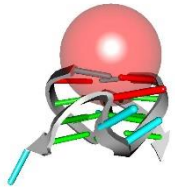
5LIG	1	G-Quadruplex formed at the 5'-end of NHEIII_1 Element in human c-MYC promoter bound to triangulenium based fluorescence probe DAOTA-M2	x: 31.332 y: 31.494 z: 27.882	15	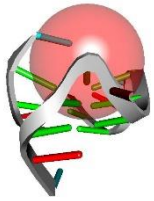
5LIG	2	G-Quadruplex formed at the 5'-end of NHEIII_1 Element in human c-MYC promoter bound to triangulenium based fluorescence probe DAOTA-M2	x: 21.082 y: 22.526 z: 20.427	15	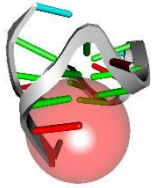

SUPPORTING DATA

5LS8	1	Light-activated ruthenium complex bound to a DNA quadruplex	x: 23.146 y: 30.753 z: 2.864	15	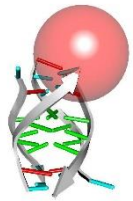
5LS8	2	Light-activated ruthenium complex bound to a DNA quadruplex	x: 21.549 y: 27.984 z: 10.919	15	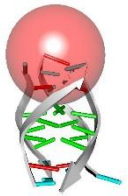
5LS8	3	Light-activated ruthenium complex bound to a DNA quadruplex	x: 19.415 y: 18.982 z: 2.228	15	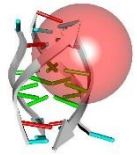
5LS8	4	Light-activated ruthenium complex bound to a DNA quadruplex	x: 11.599 y: 5.311 z: 11.487	15	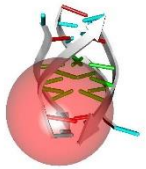

SUPPORTING DATA

5MVB	1	Solution structure of a human G-Quadruplex hybrid-2 form in complex with a Gold-ligand	x: -4.387 y: -0.927 z: 3.386	15	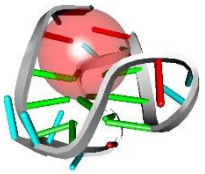
5V3F	1	Co-crystal structure of the fluorogenic RNA Mango	x: 8.285 y: 76.333 z: 154.051	15	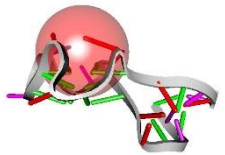
5W77	1	Solution structure of the MYC G-quadruplex bound to small molecule DC-34	x: 28.258 y: 4.461 z: 6.032	15	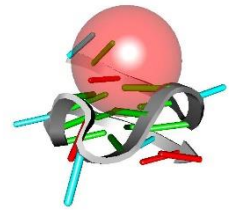
5W77	2	Solution structure of the MYC G-quadruplex bound to small molecule DC-34	x: 36.693 y: -0.914 z: -6.17	15	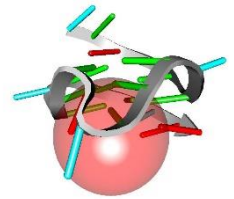

SUPPORTING DATA

5Z80	1	Solution structure for the 1:1 complex of a platinum(II)-based tripod bound to a hybrid-1 human telomeric G-quadruplex	x: -6.181 y: -0.394 z: -2.117	20	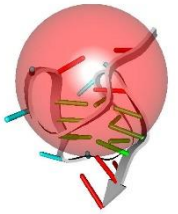
5Z8F	1	Solution structure for the unique dimeric 4:2 complex of a platinum(II)-based tripod bound to a hybrid-1 human telomeric G-quadruplex	x: -8.913 y: -3.167 z: 0.318	20	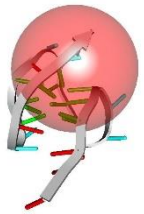
5Z8F	2	Solution structure for the unique dimeric 4:2 complex of a platinum(II)-based tripod bound to a hybrid-1 human telomeric G-quadruplex	x: -24.882 y: -2.014 z: -1.619	20	
6C63	1	Crystal Structure of the Mango-II Fluorescent Aptamer Bound to TO1-Biotin	x: 7.999 y: 32.542 z: -20.743	15	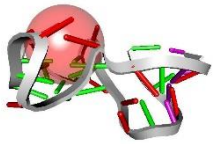

SUPPORTING DATA

6C64	1	Crystal Structure of the Mango-II Fluorescent Aptamer Bound to TO3-Biotin	x: 7.566 y: 34.962 z: -21.916	15	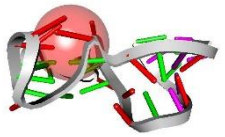
6C65	1	Crystal Structure of the Mango-II-A22U Fluorescent Aptamer Bound to TO1-Biotin	x: 8.103 y: 32.177 z: -21.022	15	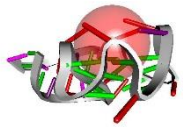
6CCW	1	Hybrid-2 form Human Telomeric G Quadruplex in Complex with Epiberberine	x: -2.028 y: 6.237 z: 0.635	15	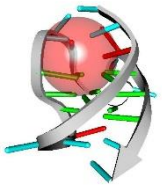
6E81	1	Crystal structure of the Corn aptamer in complex with ThT	x: 11.81 y: 52.972 z: 28.461	15	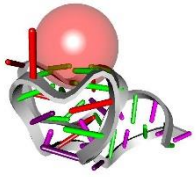

SUPPORTING DATA

6E82	1	Crystal structure of the Corn aptamer mutant A14U in complex with ThT	x: 11.647 y: 53.119 z: 28.272	15	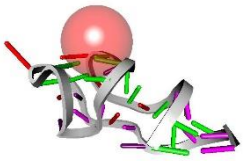
6E84	1	Crystal structure of the Corn aptamer in complex with TO	x: 12.952 y: 23.541 z: -0.929	15	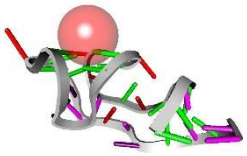
6E8S	1	Structure of the iMango-III aptamer bound to TO1-Biotin	x: -8.514 y: -69.609 z: 28.165	15	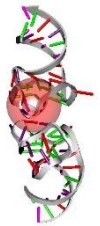
6E8T	1	Structure of the Mango-III (A10U) aptamer bound to TO1-Biotin	x: -7.859 y: 37.289 z: 74.375	15	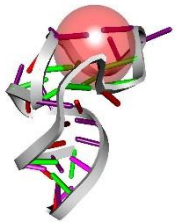

SUPPORTING DATA

6E8U	1	Structure of the Mango-III (A10U) aptamer bound to TO1-Biotin	x: 7.979 y: -4.489 z: -23.315	20	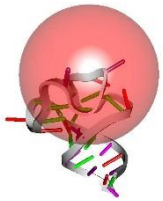
6FC9	1	The 1,8-bis(aminomethyl)anthracene and Quadruplex-duplex junction complex	x: 21.527 y: 20.957 z: 24.284	15	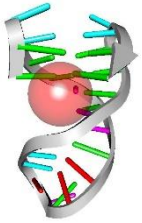
6H5R	1	Structure of the complex of a human telomeric DNA with bis(1-butyl-3-methyl-imidazole-2-ylidene) gold(I)	x: -0.228 y: 1.455 z: 1.184	15	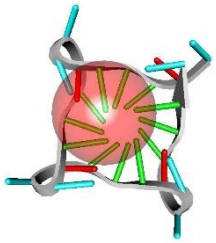
6JJ0	1	NMR structure of the 1:1 complex of a carbazole derivative BMVC bound to c-MYC G-quadruplex	x: 8.057 y: -9.4 z: -6.855	15	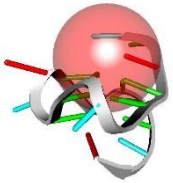

SUPPORTING DATA

6JWD	1	structure of RET G-quadruplex in complex with berberine	x: 0.794 y: 5.645 z: 1.025	15	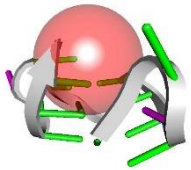
6JWE	1	structure of RET G-quadruplex in complex with colchicine	x: 2.888 y: 0.884 z: 6.584	15	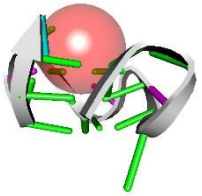
6K3Y	1	G-quadruplex complex with cyclic dinucleotide 3'-3' cGAMP	x: -3.148 y: -8.779 z: -3.716	15	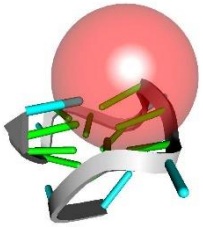
6KFI	1	NMR solution structure of the 1:1 complex of Tel26 G-quadruplex and a tripodal cationic fluorescent probe NBTE	x: -6.998 y: 0.884 z: -1.588	15	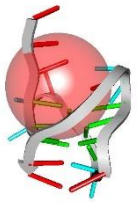

SUPPORTING DATA

6KFJ	1	NMR solution structure of the 1:1 complex of wtTel26 G-quadruplex and a tripodal cationic fluorescent probe NBTE	x: 7.688 y: -1.256 z: 3.745	15	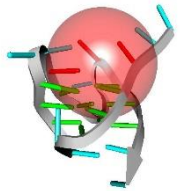
6KFL	1	Crystal structure of a two-quartet DNA G-quadruplex complexed with the porphyrin TMPyP4	x: 23.501 y: -9.321 z: -0.79	15	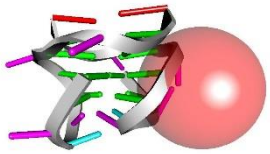
6KN4	1	HUMAN PARALLEL STRANDED 7-MER G-QUADRUPLEX COMPLEXED WITH 2 ADRIAMYCIN (DM2) MOLECULES	x: 32.184 y: 32.902 z: 37.247	15	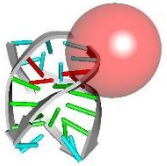
6KN4	2	HUMAN PARALLEL STRANDED 7-MER G-QUADRUPLEX COMPLEXED WITH 2 ADRIAMYCIN (DM2) MOLECULES	x: 24.372 y: 17.079 z: 12.444	15	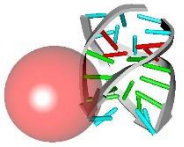

SUPPORTING DATA

6KXZ	1	HUMAN PARALLEL STRANDED 7-MER G-QUADRUPLEX COMPLEXED WITH 2 EPIRUBICIN (EPI) MOLECULES	x: 35.996 y: 30.286 z: 34.431	15	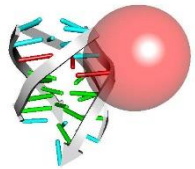
6KXZ	2	HUMAN PARALLEL STRANDED 7-MER G-QUADRUPLEX COMPLEXED WITH 2 EPIRUBICIN (EPI) MOLECULES	x: 23.974 y: 23.527 z: 8.213	15	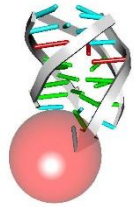
6LNZ	1	NMR solution structure of VEGF G-quadruplex bound a non-planar cyclometalated-carbene platinum(II) complex	x: 10.029 y: -24.041 z: -1.79	15	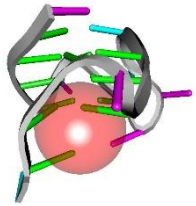
6O2L	1	NMR structure of the 2:1 complex of a carbazole derivative BMVC bound to c-MYC G-quadruplex	x: 3.292 y: -0.177 z: 3.882	15	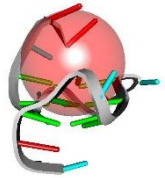

SUPPORTING DATA

6O2L	2	NMR structure of the 2:1 complex of a carbazole derivative BMVC bound to c-MYC G-quadruplex	x: 8.057 y: -9.638 z: -7.484	15	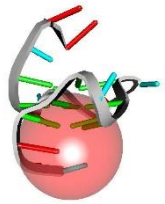
6P45	1	Crystal structure of the G-quadruplex formed by (TGGGT)4 in complex with N-methylmesoporphryin IX	x: -29.133 y: 6.944 z: 4.35	15	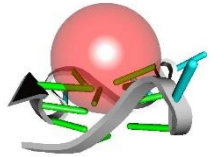
6PNK	1	Crystal structure of the G-quadruplex formed by (GGGTT)3GGG in complex with N-methylmesoporphryin IX	x: -8.572 y: 5.769 z: -34.935	15	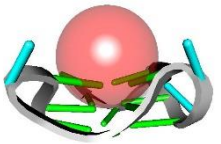
6RNL	1	L-[Ru(TAP)2(dppz)]2+ bound to the G-quadruplex forming sequence d(TAGGGTT)	x: 1.884 y: 2.379 z: -14.83	15	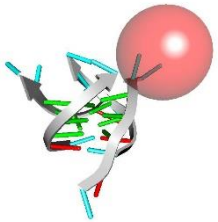

SUPPORTING DATA

6RNL	2	L-[Ru(TAP)2(dppz)]2+ bound to the G-quadruplex forming sequence d(TAGGGTT)	x: -9.305 y: -1.832 z: -12.177	15	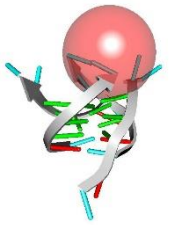
6RNL	3	L-[Ru(TAP)2(dppz)]2+ bound to the G-quadruplex forming sequence d(TAGGGTT)	x: -20.039 y: 0.21 z: -10.069	15	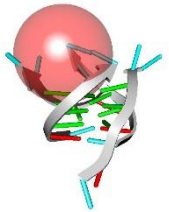
6RNL	4	L-[Ru(TAP)2(dppz)]2+ bound to the G-quadruplex forming sequence d(TAGGGTT)	x: -29.375 y: -4.428 z: -7.878	15	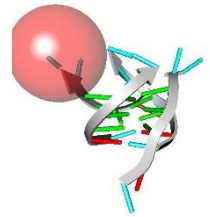
6S15	1	Pyridine derivative of the natural alkaloid Berberine as Human Telomeric G-quadruplex Binder	x: -0.835 y: -20.139 z: 5.478	15	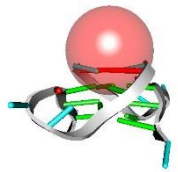

SUPPORTING DATA

6V0L	1	PDGFR-b Promoter Forms a G-Vacancy Quadruplex that Can be Complemented by dGMP: Molecular Structure and Recognition of Guanine Derivatives and Metabolites	x: 29.854 y: 27.842 z: 19.102	15	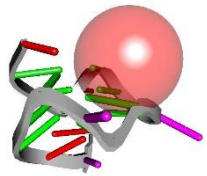
6V9B	1	Co-crystal structure of the fluorogenic Mango-IV homodimer bound to TO1-Biotin	x: 40.822 y: -1.75 z: -6.006	15	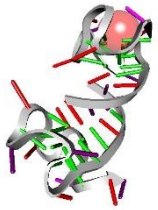
6V9B	2	Co-crystal structure of the fluorogenic Mango-IV homodimer bound to TO1-Biotin	x: 6.874 y: -11.639 z: -36.737	15	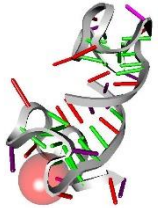
6V9B	3	Co-crystal structure of the fluorogenic Mango-IV homodimer bound to TO1-Biotin	x: 8.504 y: -11.398 z: -33.378	15	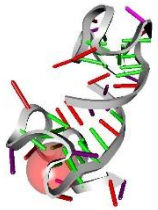

SUPPORTING DATA

6V9D	1	Co-crystal structure of the fluorogenic Mango-IV homodimer bound to TO1-Biotin	x: 19.703 y: 30.545 z: 17.212	15	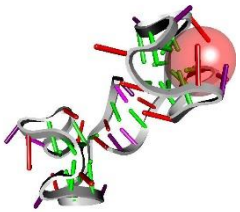
6V9D	2	Co-crystal structure of the fluorogenic Mango-IV homodimer bound to TO1-Biotin	x: 13.617 y: 0.094 z: -16.02	15	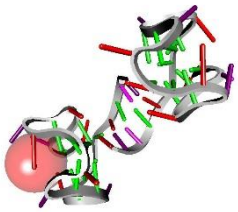
6V9D	3	Co-crystal structure of the fluorogenic Mango-IV homodimer bound to TO1-Biotin	x: 14.54 y: 2.003 z: -12.94	15	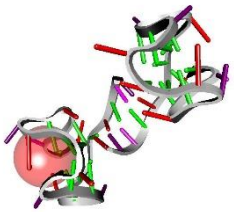
6XCL	1	Crystal Structure of human telomeric DNA G-quadruplex in complex with a novel platinum(II) complex	x: 19.152 y: -14.951 z: 8.818	15	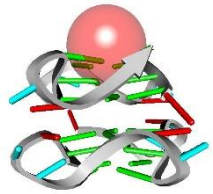

SUPPORTING DATA

6XCL	2	Crystal Structure of human telomeric DNA G-quadruplex in complex with a novel platinum(II) complex	x: 16.176 y: -27.743 z: 8.895	15	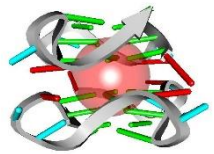

SUPPORTING DATA

Table S2 Receptor-ligand complex information

Ligand ID	PDB ID	Method	Reference
G4L8336	1O0K	X-RAY DIFFRACTION	Clark, G.R., Pytel, P.D., Squire, C.J., Neidle, S. Structure of the First Parallel DNA Quadruplex-drug Complex Journal of the American Chemical Society 10.1021/ja0297988 (2003)
G4L7743	1NZM	SOLUTION NMR	Gavathiotis, E., Heald, R.A., Stevens, M.F.G., Searle, M.S. Drug Recognition and Stabilisation of the Parallel-stranded DNA Quadruplex d(TTAGGGT)4 Containing the Human Telomeric Repeat Journal of Molecular Biology 10.1016/j.jmb.2003.09.018 (2003)
G4L0073	2A5R	SOLUTION NMR	Phan, A.T., Kuryavyi, V., Gaw, H.Y., Patel, D.J. Small-molecule interaction with a five-guanine-tract G-quadruplex structure from the human MYC promoter. Nature Chemical Biology 10.1038/nchembio723 (2005)
G4L0073	2HRI	X-RAY DIFFRACTION	Parkinson, G.N., Ghosh, R., Neidle, S. Structural basis for binding of porphyrin to human telomeres. Biochemistry 10.1021/bi062244n (2007)
G4L7462	2JT7	SOLUTION NMR	Martino, L., Virno, A., Pagano, B., Virgilio, A., Di Micco, S., Galeone, A., Giancola, C., Bifulco, G., Mayol, L., Randazzo, A. Structural and thermodynamic studies of the interaction of distamycin A with the

			parallel quadruplex structure [d(TGGGGT)]4 Journal of the American Chemical Society 10.1021/ja075710k (2007)
G4L6644	2L7V	SOLUTION NMR	Dai, J., Carver, M., Hurley, L.H., Yang, D. Solution Structure of a 2:1 Quindoline-c-MYC G-Quadruplex: Insights into G-Quadruplex-Interactive Small Molecule Drug Design. Journal of the American Chemical Society 10.1021/ja205646q (2011)
G4L1056	2MGN	SOLUTION NMR	Chung, W.J., Heddi, B., Hamon, F., Teulade-Fichou, M.P., Phan, A.T. Solution Structure of a G-quadruplex Bound to the Bisquinolinium Compound Phen-DC3. Angewandte Chemie International Edition 10.1002/anie.201308063 (2014)
G4L7849	2MS6	SOLUTION NMR	Tawani, A., Kumar, A. Structural Insight into the interaction of Flavonoids with Human Telomeric Sequence Scientific Reports 10.1038/srep17574 (2015)
G4L7849	2N6C	SOLUTION NMR	Kumar, A., Tawani, A. Solution structure for quercetin complexed with c-myc G-quadruplex DNA To be published ()
G4L6191	3CCO	X-RAY DIFFRACTION	Parkinson, G.N., Cuenca, F., Neidle, S. Topology conservation and loop flexibility in quadruplex-drug recognition: crystal structures of inter- and intramolecular telomeric DNA quadruplex-drug complexes Journal of Medicinal Chemistry

			10.1016/j.jmb.2008.06.022 (2008)
G4L6191	3CDM	X-RAY DIFFRACTION	Parkinson, G.N., Cuenca, F., Neidle, S. Topology conservation and loop flexibility in quadruplex-drug recognition: crystal structures of inter- and intramolecular telomeric DNA quadruplex-drug complexes Journal of Medicinal Chemistry 10.1016/j.jmb.2008.06.022 (2008)
G4L1041	3R6R	X-RAY DIFFRACTION	Bazzicalupi, C., Ferraroni, M., Bilia, A.R., Scheggi, F., Gratteri, P. The crystal structure of human telomeric DNA complexed with berberine: an interesting case of stacked ligand to G-tetrad ratio higher than 1:1. Nucleic Acids Research 10.1093/nar/gks1001 (2013)
G4L2016	3SC8	X-RAY DIFFRACTION	Collie, G.W., Promontorio, R., Hampel, S.M., Micco, M., Neidle, S., Parkinson, G.N. Structural basis for telomeric g-quadruplex targeting by naphthalene diimide ligands. Journal of the American Chemical Society 10.1021/ja2102423 (2012)
G4L8336	3TVB	X-RAY DIFFRACTION	Clark, G.R., Pytel, P.D., Squire, C.J. The high-resolution crystal structure of a parallel intermolecular DNA G-4 quadruplex/drug complex employing syn glycosyl linkages. Nucleic Acids Research 10.1093/nar/gks193 (2012)
G4L2017	3T5E	X-RAY DIFFRACTION	Collie, G.W., Promontorio, R., Hampel, S.M., Micco, M., Neidle, S., Parkinson, G.N. Structural basis for telomeric g-quadruplex targeting by naphthalene diimide ligands. Journal of the American Chemical Society 10.1021/ja2102423 (2012)
G4L7173	3UYH	X-RAY DIFFRACTION	Micco, M., Collie, G.W., Dale, A.G., Ohnmacht, S.A., Pazitna, I., Gunaratnam, M.,

			Reszka, A.P., Neidle, S. Structure-based design and evaluation of naphthalene diimide g-quadruplex ligands as telomere targeting agents in pancreatic cancer cells. Journal of Medicinal Chemistry 10.1021/jm301899y (2013)
G4L7173	4DA3	X-RAY DIFFRACTION	Micco, M., Collie, G.W., Dale, A.G., Ohnmacht, S.A., Pazitna, I., Gunaratnam, M., Reszka, A.P., Neidle, S. Structure-based design and evaluation of naphthalene diimide g-quadruplex ligands as telomere targeting agents in pancreatic cancer cells. Journal of Medicinal Chemistry 10.1021/jm301899y (2013)
G4L2016	4DAQ	X-RAY DIFFRACTION	Micco, M., Collie, G.W., Dale, A.G., Ohnmacht, S.A., Pazitna, I., Gunaratnam, M., Reszka, A.P., Neidle, S. Structure-based design and evaluation of naphthalene diimide g-quadruplex ligands as telomere targeting agents in pancreatic cancer cells. Journal of Medicinal Chemistry 10.1021/jm301899y (2013)
G4L0208	4L0A	X-RAY DIFFRACTION	Russo Krauss, I., Parkinson, G.N., Merlino, A., Mattia, C.A., Randazzo, A., Novellino, E., Mazzarella, L., Sica, F. A regular thymine tetrad and a peculiar supramolecular assembly in the first crystal structure of an all-LNA G-quadruplex Acta Crystallographica. Section D: Biological Crystallography 10.1107/S1399004713028095 (2014)
G4L7467	5CCW	X-RAY DIFFRACTION	Bazzicalupi, C., Ferraroni, M., Papi, F., Massai, L., Bertrand, B., Messori, L., Gratteri, P., Casini, A.

			Determinants for Tight and Selective Binding of a Medicinal Dicarbene Gold(I) Complex to a Telomeric DNA G-Quadruplex: a Joint ESI MS and XRD Investigation. Angewandte Chemie International Edition 10.1002/anie.201511999 (2016)
G4L9371	5HIX	X-RAY DIFFRACTION	Mandal, P.K., Baptiste, B., Langlois d'Estaintot, B., Kauffmann, B., Huc, I. Multivalent Interactions between an Aromatic Helical Foldamer and a DNA G-Quadruplex in the Solid State. Chembiochem 10.1002/cbic.201600281 (2016)
G4L7634	5LIG	SOLUTION NMR	Kotar, A., Wang, B., Shivalingam, A., Gonzalez-Garcia, J., Vilar, R., Plavec, J. NMR Structure of a Triangulenium-Based Long-Lived Fluorescence Probe Bound to a G-Quadruplex. Angewandte Chemie International Edition 10.1002/anie.201606877 (2016)
G4L7775	4P1D	X-RAY DIFFRACTION	Ferraroni, M., Bazzicalupi, C., Gratteri, P., Bilia, A.R., Sissi, C. Crystal Structure of the complex of a bimolecular human telomeric DNA with Coptisine To be published ()
G4L8206	5LS8	X-RAY DIFFRACTION	McQuaid, K., Abell, H., Gurung, S.P., Allan, D.R., Winter, G., Sorensen, T., Cardin, D.J., Brazier, J.A., Cardin, C.J., Hall, J.P. Structural Studies Reveal Enantiospecific Recognition of a DNA G-Quadruplex by a Ruthenium Polypyridyl Complex. Angewandte Chemie International Edition 10.1002/anie.201814502 (2019)

SUPPORTING DATA

G4L9052	5W77	SOLUTION NMR	Calabrese, D.R., Chen, X., Leon, E.C., Gaikwad, S.M., Phyo, Z., Hewitt, W.M., Alden, S., Hilimire, T.A., He, F., Michalowski, A.M., Simmons, J.K., Saunders, L.B., Zhang, S., Connors, D., Walters, K.J., Mock, B.A., Schneekloth Jr., J.S. Chemical and structural studies provide a mechanistic basis for recognition of the MYC G-quadruplex. Nature Communications 10.1038/s41467-018-06315-w (2018)
G4L9206	5Z8F	SOLUTION NMR	Liu, W., Zhong, Y.F., Liu, L.Y., Shen, C.T., Zeng, W., Wang, F., Yang, D., Mao, Z.W. Solution structures of multiple G-quadruplex complexes induced by a platinum(II)-based tripod reveal dynamic binding Nature Communications 10.1038/s41467-018-05810-4 (2018)
G4L7774	6CCW	SOLUTION NMR	Lin, C., Wu, G., Wang, K., Onel, B., Sakai, S., Shao, Y., Yang, D. Molecular Recognition of the Hybrid-2 Human Telomeric G-Quadruplex by Epiberberine: Insights into Conversion of Telomeric G-Quadruplex Structures. Angewandte Chemie International Edition 10.1002/anie.201804667 (2018)
G4L7369	6E81	X-RAY DIFFRACTION	Sjekloca, L., Ferre-D'Amare, A.R. Binding between G Quadruplexes at the Homodimer Interface of the Corn RNA Aptamer Strongly Activates Thioflavin T Fluorescence. Cell Chemical Biology 10.1016/j.chembiol.2019.04.012 (2019)
G4L7369	6E82	X-RAY DIFFRACTION	Sjekloca, L., Ferre-D'Amare, A.R. Binding between G Quadruplexes at the Homodimer Interface of the Corn RNA

			Aptamer Strongly Activates Thioflavin T Fluorescence. Cell Chemical Biology 10.1016/j.chembiol.2019.04.012 (2019)
G4L8065	6E84	X-RAY DIFFRACTION	Sjekloca, L., Ferre-D'Amare, A.R. Binding between G Quadruplexes at the Homodimer Interface of the Corn RNA Aptamer Strongly Activates Thioflavin T Fluorescence. Cell Chemical Biology 10.1016/j.chembiol.2019.04.012 (2019)
G4L9017	6H5R	X-RAY DIFFRACTION	Guarra, F., Marzo, T., Ferraroni, M., Papi, F., Bazzicalupi, C., Gratteri, P., Pescitelli, G., Messori, L., Biver, T., Gabbiani, C. Interaction of a gold(i) dicarbene anticancer drug with human telomeric DNA G-quadruplex: solution and computationally aided X-ray diffraction analysis. Dalton Transactions 10.1039/c8dt03607a (2018)
G4L7307	6JJ0	SOLUTION NMR	Liu, W., Lin, C., Wu, G., Dai, J., Chang, T.C., Yang, D. Structures of 1:1 and 2:1 complexes of BMVC and MYC promoter G-quadruplex reveal a mechanism of ligand conformation adjustment for G4-recognition. Nucleic Acids Research 10.1093/nar/gkz1015 (2019)
G4L0073	6JJI	X-RAY DIFFRACTION	Zhang, Y., El Omari, K., Duman, R., Liu, S., Haider, S., Wagner, A., Parkinson, G.N., Wei, D. Native de novo structural determinations of non-canonical nucleic acid motifs by X-ray crystallography at long wavelengths. Nucleic Acids Research 10.1093/nar/gkaa439 (2020)

SUPPORTING DATA

G4L1041	6JWD	SOLUTION NMR	Wang, F., Wang, C., Liu, Y., Lan, W., Han, H., Wang, R., Huang, S., Cao, C. Colchicine selective interaction with oncogene RET G-quadruplex revealed by NMR. Chemical Communications 10.1039/d0cc00221f (2020)
G4L1336	6JWE	SOLUTION NMR	Wang, F., Wang, C., Liu, Y., Lan, W., Han, H., Wang, R., Huang, S., Cao, C. Colchicine selective interaction with oncogene RET G-quadruplex revealed by NMR. Chemical Communications 10.1039/d0cc00221f (2020)
G4L0073	6KFL	X-RAY DIFFRACTION	Zhang, Y.S., Parkinson, G.N., Wei, D.G. Crystal structure of a two-quartet DNA G-quadruplex complexed with the porphyrin TMPyP4 To be published ()
G4L7500	6KN4	SOLUTION NMR	Barthwal, R., Raje, S., Pandav, K. Structural basis for stabilization of human telomeric G-quadruplex [d-(TTAGGGT)] 4 by anticancer drug adriamycin. Journal of Biomolecular Structure & Dynamics 10.1080/07391102.2020.1730969 (2021)
G4L7307	6O2L	SOLUTION NMR	Liu, W., Lin, C., Wu, G., Dai, J., Chang, T.C., Yang, D. Structures of 1:1 and 2:1 complexes of BMVC and MYC promoter G-quadruplex reveal a mechanism of ligand conformation adjustment for G4-recognition. Nucleic Acids Research 10.1093/nar/gkz1015 (2019)
G4L8206	6RNL	X-RAY DIFFRACTION	McQuaid, K., Hall, J.P., Baumgaertner, L., Cardin, D.J., Cardin, C.J. Three thymine/adenine binding modes of the ruthenium complex

SUPPORTING DATA

			Lambda-[Ru(TAP)2(dppz)]2+to the G-quadruplex forming sequence d(TAGGGTT) shown by X-ray crystallography. Chemical Communications 10.1039/c9cc04316k (2019)
G4L1041	6S15	X-RAY DIFFRACTION	Papi, F., Bazzicalupi, C., Ferraroni, M., Ciolli, G., Lombardi, P., Khan, A.Y., Kumar, G.S., Gratteri, P. Pyridine Derivative of the Natural Alkaloid Berberine as Human Telomeric G4-DNA Binder: A Solution and Solid-State Study. ACS Medicinal Chemistry Letters 10.1021/acsmedchemlett.9b00516 (2020)
G4L7402	6SX3	SOLUTION NMR	Kotar, A., Kocman, V., Plavec, J. Intercalation of a Heterocyclic Ligand between Quartets in a G-Rich Tetrahelical Structure. Chemistry 10.1002/chem.201904923 (2020)
G4L9651	7KLP	X-RAY DIFFRACTION	Li, K., Yatsunyk, L., Neidle, S. Water spines and networks in G-quadruplex structures. Nucleic Acids Research 10.1093/nar/gkaa1177 (2021)
G4L0174	3CE5	X-RAY DIFFRACTION	Campbell, N.H., Parkinson, G.N., Reszka, A.P., Neidle, S. Structural basis of DNA quadruplex recognition by an acridine drug. J Am Chem Soc 10.1021/ja8016973 (2008)
G4L1584	3MIJ	X-RAY DIFFRACTION	Collie, G.W., Sparapani, S., Parkinson, G.N., Neidle, S. Structural basis of telomeric RNA quadruplex-acridine ligand recognition.

SUPPORTING DATA

			J Am Chem Soc 10.1021/ja109767y